Probing grand unified theories with cosmic-ray, gamma-ray, and neutrino astrophysics

Günter Sigl and Sangjin Lee

Department of Astronomy & Astrophysics, Enrico Fermi Institute, The University of Chicago, Chicago, Illinois 60637-1433

Pijushpani Bhattacharjee

Laboratory for High Energy Astrophysics, Code 661, NASA/Goddard Space Flight Center, Greenbelt, Maryland 20771
and Indian Institute of Astrophysics, Bangalore-560 034, India

Shigeru Yoshida

Institute for Cosmic Ray Research, University of Tokyo, Tanashi, Tokyo 188-8502, Japan

We explore scenarios where the highest energy cosmic rays are produced by new particle physics near the grand unification scale. Using detailed numerical simulations of extragalactic nucleon, γ-ray, and neutrino propagation, we show the existence of an interesting parameter range for which such scenarios may explain part of the data and are consistent with all observational constraints. A combination of proposed observatories for ultra-high energy cosmic rays, neutrino telescopes of $\gtrsim$ few kilometer scale, and γ-ray astrophysics instruments, should be able to test these scenarios. In particular, for neutrino masses in the eV range, exclusive neutrino decay modes of superheavy particles can give rise to neutrino fluxes comparable to those predicted in models of active galactic nuclei. [S0556-2821(99)06202-5]

I. INTRODUCTION

The highest energy cosmic ray (HECR) events observed above 100 EeV ($1\,\text{EeV}=10^{18}\,\text{eV}$) [1,2] are difficult to explain within conventional models involving first order Fermi acceleration of charged particles at astrophysical shocks [3]. It is hard to accelerate protons and heavy nuclei up to such energies even in the most powerful astrophysical objects [4] such as radio galaxies and active galactic nuclei. Also, nucleons above $\simeq 70\,\text{EeV}$ lose energy drastically due to photopion production on the cosmic microwave background (CMB)—the Greisen-Zatsepin-Kuzmin (GZK) effect [5]—which limits the distance to possible sources to less than $\simeq 100\,\text{Mpc}$ [6]. Heavy nuclei are photodisintegrated in the CMB within a few Mpc [7]. There are no obvious astronomical sources within $\simeq 100\,\text{Mpc}$ of Earth.

A way around these difficulties is to suppose that the HECRs are created directly as decay or interaction products of particles with masses much higher than the observed energies, rather than being accelerated from lower energies. In the current versions of such ''top-down'' (TD) scenarios, predominantly γ-rays and neutrinos are initially produced at ultra-high energies (UHEs) by the decay of supermassive elementary ''X'' particles related to some grand unified theory (GUT). Such X particles could be released from topological defect relics of phase transitions which might have been caused by spontaneous breaking of GUT symmetries in the early Universe [8]. TD models of this type are attractive because they predict injection spectra which are considerably harder than shock acceleration spectra and which can extend to an energy of $\sim 10^{16}\,\text{GeV}$, typical in GUTs. The absence of obviously identifiable astronomical sources is also not a problem because the (sources of) X particles need not be associated with any visible or otherwise active astrophysical sources.

There has been considerable discussion in the literature whether the γ-ray, nucleon, and neutrino fluxes predicted by TD scenarios are consistent with all the relevant observational data and constraints at various energies [9–13]. The absolute flux levels predicted by TD models are in general uncertain. While some (though perhaps not all) processes involving cosmic strings seem to yield negligibly low fluxes [14], other processes such as those involving annihilation of magnetic monopole-antimonopole pairs [15,16], cosmic necklaces [17], and possible [18] (but currently controversial [19]) direct emission of X particles from cosmic strings can [20,21], for reasonable values of parameters, yield X particles at rates sufficient to explain the observed HECR flux.

In this work, instead of trying to calculate the absolute fluxes in specific TD models, we use the strategy to numerically calculate the fluxes of nucleons, γ-rays, and neutrinos, ''optimally'' normalize them to match data and constraints, and discuss the feasibility and consequences of a set of most ''favorable'' ranges of the relevant parameters implied by our calculations.

A major new feature of our calculations is that our ''all particle'' propagation code includes the feedback effect of neutrino cascading on the electromagnetic and hadronic channels in a fully self-consistent manner (see below). In addition, spurred by recent experimental indications of a possible small neutrino mass, we include in our calculations the effects of a small neutrino mass ($\sim$eV) and the consequent Z-boson resonance in the interaction of UHE neutrinos with the thermal neutrinos.

II. TOP-DOWN MODELS

The X particles released from topological defects could be gauge bosons, Higgs bosons, superheavy fermions, etc., depending on the specific GUT. These X particles would have

a mass m_X comparable to the symmetry breaking scale and would rapidly decay into leptons and/or quarks of roughly comparable energy. We will accordingly consider several possibilities for the decay products. Prior calculations were restricted to decay into only quarks. The quarks interact strongly and hadronize into nucleons (N's) and pions, the latter decaying in turn into γ-rays, electrons, and neutrinos. Given the X particle production rate, dn_X/dt, the effective injection spectrum of particle species a ($a = \gamma, N, e^{\pm}, \nu$) via the hadronic channel can be written as $(dn_X/dt)(2/m_X)(dN_a/dx)$, where $x \equiv 2E/m_X$, and dN_a/dx is the relevant fragmentation function (FF).

We adopt the local parton hadron duality (LPHD) approximation [22] according to which the total hadronic FF, dN_h/dx, is taken to be proportional to the spectrum of the partons (quarks/gluons) in the parton cascade (which is initiated by the quark through perturbative QCD processes) after evolving the parton cascade to a stage where the typical transverse momentum transfer in the QCD cascading processes has come down to $\sim R^{-1} \sim$ few hundred MeV, where R is a typical hadron size. The parton spectrum is obtained from solutions of the standard QCD evolution equations in a modified leading logarithmic approximation (MLLA) which provides good fits to accelerator data at CERN e^+e^- collider LEP energies [22]. We also use a recently suggested generalization of the MLLA spectrum that includes the effects of supersymmetry [23]. We abbreviate the above two cases as ''no-SUSY'' and ''SUSY,'' respectively. The difference in the results for these two choices will be a measure of the uncertainty associated with the FF. Within the LPHD hypothesis, the pions and nucleons after hadronization have essentially the same spectrum. The LPHD does not, however, fix the relative abundance of pions and nucleons after hadronization. Motivated by accelerator data, we assume the nucleon content f_N of the hadrons to be in the range 3–10 %, and the rest pions distributed equally among the three charge states. According to recent Monte Carlo simulations [24], the nucleon-to-pion ratio may be significantly higher in certain ranges of x values at the extremely high energies of interest here. Unfortunately, however, because of the very nature of these Monte Carlo calculations, it is difficult to understand the precise physical reason for the unexpectedly high baryon yield relative to mesons. While more of these Monte Carlo calculations of the relevant FFs in the future will hopefully clarify the situation, we will use here the range of f_N ~ 3–10 % mentioned above. The standard pion decay spectra then give the injection spectra of γ-rays, electrons, and neutrinos.

The X particle injection rate is assumed to be spatially uniform and in the matter-dominated era can be parametrized as $dn_X/dt \propto t^{-4+p}$ [8], where p depends on the specific defect scenario. In this paper we focus on the case $p = 1$ which is representative of a number of specific TD processes involving ordinary cosmic strings [25,18,20,21], necklaces [17] and magnetic monopoles [16]. Finally, we assume that the X particles are nonrelativistic at decay.

III. NUMERICAL SIMULATIONS

The γ-rays and electrons produced by X particle decay initiate electromagnetic (EM) cascades on low energy radia-

tion fields such as the CMB. The high energy photons undergo electron-positron pair production (PP) ($\gamma \gamma_b \rightarrow e^-e^+$), and at energies below $\sim 10^{14}$ eV they interact mainly with the universal infrared and optical (IR/O) backgrounds, while above ~ 100 EeV they interact mainly with the universal radio background (URB). In the Klein-Nishina regime, where the center of mass energy is large compared to the electron mass, one of the outgoing particles usually carries most of the initial energy. This ''leading'' electron (positron) in turn can transfer almost all of its energy to a background photon via inverse Compton scattering (ICS) ($e \gamma_b \rightarrow e' \gamma$). EM cascades are driven by this cycle of PP and ICS. The energy degradation of the ''leading'' particle in this cycle is slow, whereas the total number of particles grows exponentially with time. This makes a standard Monte Carlo treatment difficult. We have therefore used an implicit numerical scheme to solve the relevant kinetic equations. A detailed account of our transport equation approach is in Ref. [26]. We include all EM interactions that influence the γ-ray spectrum in the energy range 10^8 eV $< E < 10^{25}$ eV, namely PP, ICS, triplet pair production (TPP) ($e \gamma_b \rightarrow ee^-e^+$), and double pair production ($\gamma \gamma_b \rightarrow e^-e^+e^-e^+$), as well as synchrotron losses of electrons in the large scale extragalactic magnetic field (EGMF).

Similarly to photons, UHE neutrinos give rise to neutrino cascades in the primordial neutrino background via exchange of W and Z bosons [27,28]. Besides the secondary neutrinos which drive the neutrino cascade, the W and Z decay products include charged leptons and quarks which in turn feed into the EM and hadronic channels. Neutrino interactions become especially significant if the relic neutrinos have masses m_ν in the eV range and thus constitute hot dark matter, because the Z boson resonance then occurs at an UHE neutrino energy $E_{res} = 4 \times 10^{21}$ (eV/m_ν) eV. In fact, this has been proposed as a significant source of HECRs [29,30]. Motivated by recent experimental evidence for neutrino mass we assumed a mass of 1 eV for all three neutrino flavors and implemented the relevant W boson interactions in the t-channel and the Z boson exchange via the t- and s-channels. Hot dark matter is also expected to cluster, potentially increasing secondary γ-ray and nucleon production [29,30]. This influences mostly scenarios where X decays into neutrinos only. We parametrize massive neutrino clustering by a length scale l_ν and an overdensity f_ν over the average density $\bar{n}_\nu$. The Fermi distribution with a velocity dispersion v yields $f_\nu \lesssim v^3 m_\nu^3/(2\pi)^{3/2}/\bar{n}_\nu \simeq 330 (v/500 \text{ km sec}^{-1})^3 (m_\nu/\text{eV})^3$ [31]. Therefore, values of $l_\nu \simeq$ few Mpc and $f_\nu \simeq 20$ are conceivable on the local Supercluster scale [30].

The relevant nucleon interactions implemented are pair production by protons ($p \gamma_b \rightarrow pe^-e^+$), photoproduction of single or multiple pions ($N \gamma_b \rightarrow N n\pi$, $n \geq 1$), and neutron decay. In TD scenarios, the particle injection spectrum is generally dominated by the ''primary'' γ-rays and neutrinos over nucleons. These primary γ-rays and neutrinos are produced by the decay of the primary pions resulting from the hadronization of quarks that come from the decay of the X particles. The contribution of secondary γ-rays, electrons, and neutrinos from decaying pions that are subsequently pro-

TABLE I. Some viable $p=1$ TD scenarios explaining HECRs at least above 100 EeV.

m_X[a]	Fig.	URB	EGMF[b]	FF	f_N	Mode	Q^{0c}	$\lesssim$GZK[d]	$\gtrsim$GZK[d]
10^{13}	4	$f_\nu l_\nu \gtrsim 400$ Mpc for high URB, no EGMF[e]				$\nu\nu$	$\lesssim 31$	γ	γ
	3	high	any	no-SUSY	10%	qq	1.4	N	N
		$\lesssim$med	$\lesssim 10^{-11}$	no-SUSY	$\lesssim 10\%$	qq	1.4	N	γ
	3	high	$\lesssim 10^{-11}$	no-SUSY	10%	ql	0.88	N	γ
		$\lesssim$med	$\lesssim 10^{-11}$	any	$\lesssim 10\%$	ql	0.93	γ	γ
		any	$\lesssim 10^{-11}$	-	-	$ll,l\nu$	1.3	γ	γ
10^{14}	4	$f_\nu l_\nu \gtrsim 150$ Mpc for high URB, no EGMF[e]				$\nu\nu$	$\lesssim 19$	γ	γ
		high	any	no-SUSY	10%	qq	1.3	N	$\gamma+N,N^f$
		$\lesssim$med	$\lesssim 10^{-10}$	no-SUSY	$\lesssim 10\%$	$qq,q\nu$	1.3	$\gamma+N$	γ
		any	$\lesssim 10^{-11}$	any	$\lesssim 10\%$	ql	0.97	N	γ
		any	$\lesssim 10^{-11}$	-	-	$ll,l\nu$	1.4	γ	γ
10^{15}		$f_\nu l_\nu \gtrsim 500$ Mpc for high URB, no EGMF[e]				$\nu\nu$	$\lesssim 25$	γ	γ
		any	any	any	10%	$qq,ql,q\nu$	1.3	N	
		$\lesssim$med	$\lesssim 10^{-11}$	any	$\lesssim 10\%$	$qq,ql,q\nu$	1.3		
		any	$\lesssim 10^{-11}$	-	-	$ll,l\nu$	1.3	γ	γ
10^{16}		$f_\nu l_\nu \gtrsim 3000$ Mpc for high URB, no EGMF[e]				$\nu\nu$	$\lesssim 2.0$	γ	γ
	1, 2	high	any	SUSY	10%	qq	1.6	N	$\gamma+N,N^f$
	1, 2	high	$\lesssim 10^{-9}$	no-SUSY	10%	qq	1.3	γ,N^f	$\gamma,\gamma+N^g$
		any	$\lesssim 10^{-11}$	any	$\lesssim 10\%$	$qq,ql,q\nu$	1.9		
		$\lesssim$med	$\lesssim 10^{-11}$	-	-	$ll,l\nu$	1.6	γ	γ

[a]In GeV.

[b]In Gauss.

[c]Maximal total energy injection rate at zero redshift in $10^{-23} h$ eV cm^{-3} sec^{-1}.

[d]Dominant component of ''visible'' TD flux below and above GZK cutoff at $\simeq 70$ EeV; no entry means different composition is possible, depending on parameters.

[e]Viable for eV mass neutrinos if their overdensity f_ν over a scale l_ν obeys specified condition for the high URB and vanishing EGMF; for weaker URB the condition relaxes, for stronger EGMF it becomes more stringent.

[f]For EGMF $\gtrsim 10^{-10}$ G.

[g]For EGMF $\gtrsim 10^{-9}$ G.

duced by the interactions of nucleons with the CMB is in general negligible compared to that of the primary particles; we nevertheless include the contribution of the secondary particles in our code.

We assume a flat universe with no cosmological constant, and a Hubble constant of $h=0.65$ in units of 100 km sec^{-1} Mpc^{-1} throughout. An important difference with respect to past work is that we follow *all* produced particles in the EM, hadronic, and neutrino channel, whereas the often-used continuous energy loss (CEL) approximation (e.g., [32]) follows only the leading cascade particles. We find that the CEL approximation can significantly underestimate the cascade flux at lower energies.

The two major uncertainties in the particle transport are the intensity and spectrum of the URB, for which there exists only an estimate above a few MHz frequency [33], and the average value of the EGMF. To bracket these uncertainties we performed simulations for the observational URB estimate from Ref. [33] that has a low-frequency cutoff at 2 MHz (''minimal''), and the medium and maximal theoretical estimates from Ref. [34], as well as for EGMFs between zero and 10^{-9} G, the latter motivated by limits from Faraday rotation measurements [35]. A strong URB tends to suppress the UHE γ-ray flux by direct absorption whereas a strong

EGMF blocks EM cascading (which otherwise develops efficiently especially in a low URB) by synchrotron cooling of the electrons. For the IR/O background we used the most recent data [36].

IV. PARTICLE FLUXES

We now present results from our flux calculations for a variety of combinations of URBs, EGMFs, FFs, fractions f_N of nucleons created in quark fragmentation, and X particle decay modes. Table I identifies some of the scenarios that were found capable of explaining HECRs at least above 100 EeV, without violating any observational constraints, along with the predicted composition of the TD component below and above the GZK cutoff. The spectrum was normalized in the best possible way to explain observed HECRs as being due either to nucleon or γ-ray primaries. The flux below $\lesssim 20$ EeV is presumably due to conventional acceleration and was not fit. We remark that above 100 EeV, the best fits for the viable scenarios from Table I have acceptable likelihood significances (see Ref. [37] for details) and are consistent with the integral flux above 300 EeV estimated in Refs. [1,2], in contrast to direct fits to the observed differential flux at 300 EeV [12] which would lead to an overproduction
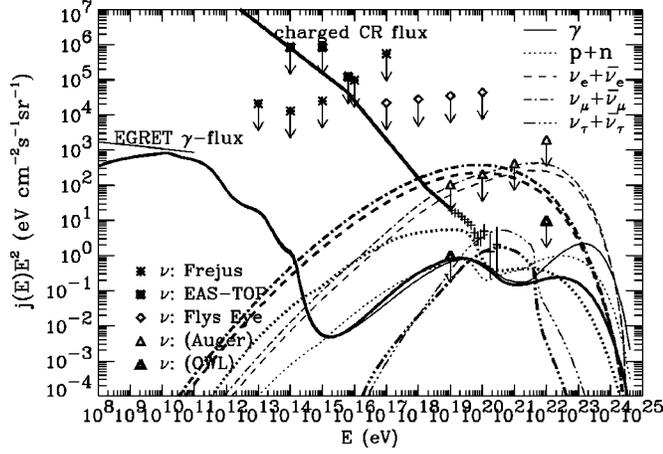
FIG. 1. Energy spectra of nucleons, γ-rays and neutrinos for the TD model with $m_X = 10^{16}$ GeV, $p = 1$, and the decay mode $X \to q + q$, assuming the high URB version and an EGMF of 10^{-10} G. Thick and thin lines represent the SUSY and no-SUSY FFs, respectively. One sigma error bars are the combined data from the Haverah Park [38], Fly's Eye [1] and AGASA [2] experiments above 10 EeV. Also shown are piecewise power law fits to the observed charged cosmic ray flux below 10 EeV, the EGRET measurement of the diffuse γ-ray flux between 30 MeV and 100 GeV [39], and experimental neutrino flux limits from Frejus [40] and Fly's Eye [41], as well as projected neutrino sensitivities of the future Pierre Auger [42] and NASA's OWL [44] projects.

of the integral flux at higher energies.

Figures 1–4 show the fluxes of some scenarios indicated in Table I, along with current observational constraints on and projected sensitivities of some future experiments to γ-ray and neutrino fluxes. This demonstrates consistency with present constraints within the normalization ambiguity. In particular, EM energy injected at high redshifts is recycled by cascading to lower energies, as can be seen in Fig. 1. TD models are therefore significantly constrained [9,10] by current limits on the diffuse γ-ray background between 30 MeV and 100 GeV [39] which acts as a ``calorimeter'' and requires $Q_{EM}^0 \lesssim 2.2 \times 10^{-23} h(3p-1)$ eV cm^{-3} sec^{-1} for the total present energy injection rate into the EM channel. On the other hand, it is not clear whether the observed diffuse background above 10 GeV can be fully accounted for by conventional sources such as unresolved blazars [45] and it has been suggested that decays of heavy particles may provide a significant contribution in this energy range [20]. As can be seen in the figures, this is also the case for the TD scenarios studied here. In these scenarios, the CMB depletes the photon flux above 100 TeV, and the IR/O background in the range 100 GeV–100 TeV, recycling it to energies below 100 GeV (see Fig. 1). However, the resulting background is *not* very sensitive to the specific IR/O background model, as was shown in Ref. [46]. Constraints from limits on CMB distortions and light element abundances from ^{4}He-photodisintegration are comparable to the bound from the directly observed γ-rays [10].

Figures 2 and 3 compare the UHE fluxes from four TD scenarios indicated in Table I. Figure 2 compares the SUSY and no-SUSY FF for $m_X = 10^{16}$ GeV, all parameters being
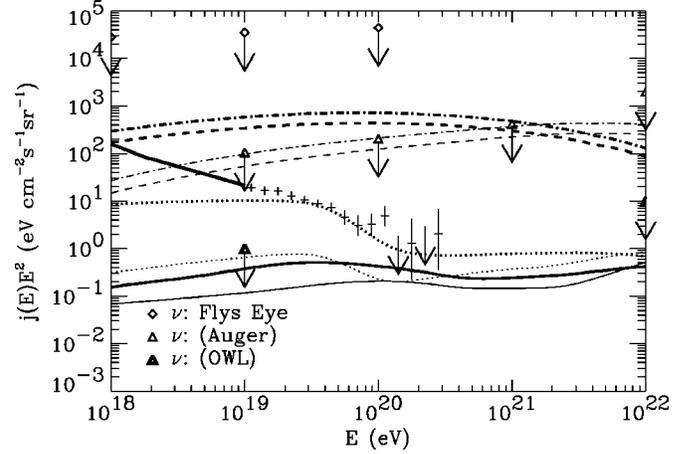
FIG. 2. The fluxes at energies above 1 EeV for the scenarios shown in Fig. 1, for an EGMF of 10^{-9} G, all other parameters being the same. The tau neutrino fluxes were omitted for clarity. The no-SUSY FF case is only marginally viable for such strong EGMF.

the same as in Fig. 1, except for an EGMF of 10^{-9} G. Figure 3 compares the two decay channels $X \to q + l$ and $X \to q + q$ for $m_X = 10^{13}$ GeV, assuming the no-SUSY FF and an EGMF of $\lesssim 10^{-11}$ G. Both figures assume the high URB and a fraction $f_N \simeq 10\%$ of nucleons created in quark fragmentation. The present energy injection rate Q_{HECR}^0 required to produce the UHE fluxes $j_a(E)$ can be estimated as

$$Q_{HECR}^0 \simeq 10^{-22} \left(\frac{E^2 j_a(E)}{\text{eV cm}^{-2} \text{sr}^{-1} \text{sec}^{-1}} \right) \left(\frac{x^2 dN_a/dx}{0.004} \right)^{-1}$$
$$\times \left(\frac{\lambda_a(E)}{10 \text{ Mpc}} \right)^{-1} \text{eV cm}^{-3} \text{sec}^{-1}, \qquad (1)$$

where $x = 2E/m_X$, $\lambda_a(E)$ is the effective attenuation length of species a, and the fiducial values are for $E = 100$ EeV and
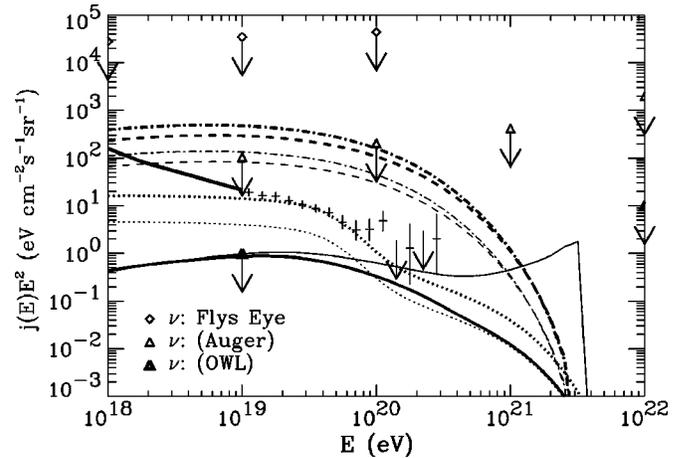
FIG. 3. Same as Fig. 2, but for $m_X = 10^{13}$ GeV, and the no-SUSY FF, assuming a vanishing EGMF. Here, the thick and thin lines represent the decay modes $X \to q + q$ and $X \to l + q$, respectively. The same normalization of the GeV γ-ray flux as in Fig. 1 was used.

the SUSY FF for $m_X = 10^{16}$ GeV. For the SUSY and no-SUSY FF, Q_{HECR}^0 turns out to be minimal around $m_X \sim 10^{15}$ GeV and 10^{14} GeV, respectively, and increases below and above that. This is confirmed by the numerical calculations, as can be seen from Figs. 2 and 3 and from Table I. We therefore conclude that for most combinations of the URB and the EGMF, the most poorly known astrophysical ingredients, one can find combinations of possible decay modes and FFs that make $p = 1$ TD models with homogeneous source distribution viable HECR explanations for 10^{13} GeV $\lesssim m_X \lesssim 10^{16}$ GeV. We note in this context that in some GUT models, certain baryon number violating decay modes involving leptons and quarks may violate limits on proton decay if m_X is too far below 10^{15} GeV, and may therefore be disfavored: see, for example Ref. [47].

The energy loss and absorption lengths for UHE nucleons and photons are short ($\lesssim 100$ Mpc). Thus, their predicted UHE fluxes are independent of cosmological evolution. The γ-ray flux below $\simeq 10^{11}$ eV, however, scales as the total X particle energy release integrated over all redshifts and increases with decreasing p [10] roughly as $1/(3p-1)$. Scenarios with $p < 1$ are therefore in general ruled out (see Figs. 1–3), whereas constant comoving injection rates ($p = 2$) are well within the limits. Since the EM flux above $\simeq 10^{22}$ eV is efficiently recycled to lower energies, the constraint on p is in general less sensitive to m_X than expected from earlier CEL-based analytical estimates [9,10].

A specific $p = 2$ scenario is realized in the case where the supermassive X particles have a lifetime longer than the age of the Universe and contribute to the cold dark matter. For superheavy long lived cold dark matter, non-thermal production in the early Universe has recently been identified as a serious possibility, either gravitationally through the effect of the expansion of the background metric on the vacuum quantum fluctuations of the X field [48–50] or during reheating at the end of inflation if the X field couples to the inflation field [51,52]. In this case, local clustering of the sources in the galactic halo has to be taken into account which provides the dominant contribution to observable fluxes [53]. As a consequence, the predicted spectra and composition just reflect the injection spectrum, and the diffuse γ-ray background at Energetic Gamma Ray Experiment Telescope (EGRET) energies is not a serious constraint.

We now turn to signatures of TD models at UHEs. The full cascade calculations predict γ-ray fluxes below 100 EeV that are a factor $\simeq 3$ and $\simeq 10$ higher than those obtained using the CEL or absorption approximation often used in the literature [54], in the case of strong and weak URB, respectively. This is also seen by comparing Eq. (1) for the γ-ray flux with the maximum energy injection rate Q_{EM}^0 allowed by the EGRET observations, which yields $\lambda_\gamma \simeq 100$ Mpc, and which is consistent with the total energy injection rates Q^0 given in Table I. Again, this shows the importance of non-leading particles in the development of unsaturated EM cascades at energies below $\sim 10^{22}$ eV. As a consequence, in all viable HECR explaining cases with only quarks among the X particle decay products, we obtain γ/nucleon ratios above 200 EeV that are $\gtrsim 0.1/f_N$ for $m_X \gtrsim 10^{15}$ GeV and about a
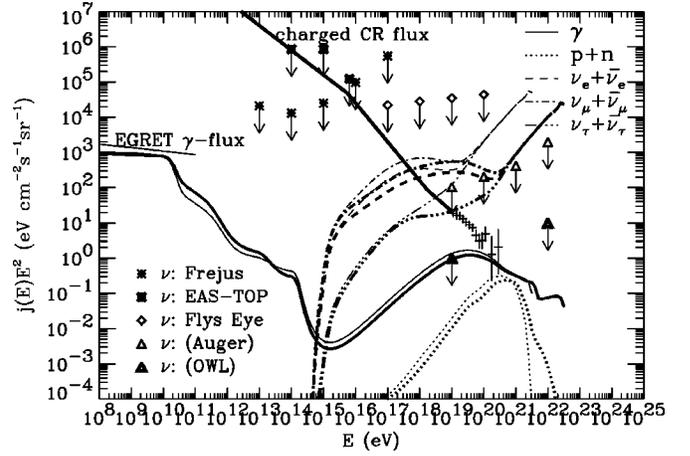
FIG. 4. Same as Fig. 1, but for the pure neutrino decay mode with no EGMF. Shown are the maximal UHE neutrino fluxes allowed by the EGRET limit for $m_X = 10^{14}$ GeV (thick lines) and $m_X = 10^{13}$ GeV (thin lines). For neutrino clustering the lower limits from Table I, required to explain HECRs, were assumed. This would correspond to overdensities of $\simeq 30$ and $\simeq 75$ over a scale $l_\nu \simeq 5$ Mpc.

factor 2 smaller for $m_X \lesssim 10^{14}$ GeV, even for the maximal URB, if the EGMF is $\lesssim 10^{-11}$ G. This ratio is about a factor of 3 higher for the decay modes containing a charged lepton. Although a γ-ray primary for the HECR events is somewhat disfavored currently [55], the compositional issue is not settled yet, but future experiments such as the Pierre Auger project [56] should be able to distinguish γ-ray and nucleon primaries and test this signature. We stress that there are viable scenarios with nucleon fluxes that are comparable with or even higher than the γ-ray flux at all energies in case of the high URB and/or for a strong EGMF, and $f_N \simeq 10\%$: see Figs. 2 and 3, and Table I. The predictions from the SUSY FF in Fig. 2 even seem able to explain all cosmic rays above $\simeq 20$ EeV by nucleon primaries. The low m_X, pure quark decay modes such as the one shown in Fig. 3 may be able to explain all cosmic rays above 10 EeV by nucleon primaries, but also tend to produce a more rapid fall off of fluxes beyond 100 EeV, which constitutes another testable signature. The γ/nucleon ratio above 100 EeV is about a factor 5 and 10 higher in the medium and minimal URB, respectively, as compared to the strong URB case, and in general decreases strongly with increasing EGMF $\gtrsim 10^{-11}$ G.

As indicated in Table I, another interesting scenario involves the pure neutrino decay modes, also shown in Fig. 4 for $m_X \lesssim 10^{14}$ GeV. Here, the γ-rays and nucleons are produced as secondaries from the interactions of these UHE neutrinos with the relic neutrinos. Because γ-rays and nucleons above 100 EeV must have been produced within a distance $\lambda_a \simeq$ few Mpc from the observer, their flux is dominantly produced by interactions with the locally clustered neutrinos if $l_\nu f_\nu \gtrsim \lambda_a$. In this case, the energy fluence in the secondaries is about $f_Z(f_\nu l_\nu/\lambda_Z)$ times the energy fluence in primary neutrinos around the Z resonance, where $f_Z \simeq 3\%$ is the fractional width of the Z and $\lambda_Z \simeq 38$ Gpc is the neutrino mean free path at the Z resonance at zero redshift. In con-

trast, at energies where the Universe is transparent for particles today, the dominant contribution to their production by UHE neutrinos comes from interactions with the unclustered relic neutrino component at high redshift. This is because for energies $E \gtrsim E_{\mathrm{res}}$, the probability for both resonant and non-resonant interaction with the relic background per redshift interval is roughly $(1+z)^{1/2} f_Z t_0 / \lambda_Z$ in the matter dominated regime, where t_0 is the age of the Universe (for $E \lesssim E_{\mathrm{res}}$ this probability decreases linearly with E). Because the Universe is opaque for γ-rays above ~ 100 TeV, this implies that the diffuse γ-ray background below some energy E is sensitive to the injection history at $z \gtrsim (100 \, \mathrm{TeV}/E)^{1/2}$. This explains why the γ-ray background is steeper below 10 GeV than in the scenarios where its dominant production is not by neutrino interactions: see Fig. 4. As a further consequence of neutrino interactions, the secondary neutrino fluxes below an energy $E \lesssim E_{\mathrm{res}}$ are sensitive to the injection history at $z \gtrsim E_{\mathrm{res}}/E$. For $p=1$ scenarios, all other fluxes are insensitive to the injection history at $z \gtrsim 100$. Since we are mainly interested in neutrino fluxes above 10 EeV and γ-ray fluxes above 100 MeV, it was therefore sufficient to integrate injection up to $z = 10^3$ which also approximately marks the transition to radiation domination. In addition, for $p=1$, the scaling of neutrino interaction rates implies that the energy content in the secondaries, and thus in particular in the low energy cascade γ-rays, constitutes a few percent of the energy in UHE neutrinos. This fixes the maximally allowed UHE neutrino flux which is shown in Fig. 4 and implies the lower limit on $l_\nu f_\nu$ given in Table I which is required if secondaries of UHE neutrino interactions are to explain HECRs. The maximal energy injection rate in neutrinos today allowed by the EGRET limit is correspondingly higher than the upper bound on Q_{EM}^0 by about a factor of 10. Observational consequences of the UHE neutrino fluxes are discussed in the following section.

The spectra predicted by scenarios where the X particles decay into more than two quanta are qualitatively similar to the ones for decay into two particles of the same type. The details, however, depend on the energy distributions of the decay products. To avoid introducing further model dependent parameters, we do not consider such refinements in the present paper as we do not consider scenarios where the X particles themselves are created with relativistic energies.

V. NEUTRINO FLUX DETECTION

In order to discuss the prospects of detectability of neutrino fluxes in TD scenarios we express the (in general energy dependent) experimental sensitivities in terms of the ice or water equivalent acceptance $A(E)$ (in units of volume times solid angle). Future neutrino telescopes of kilometer scale or larger will utilize the detection of Cherenkov radiation from muons and EM showers created in interactions of the neutrinos with nucleons either in ice or in the deep sea. Examples for experiments that aim at this effective size are the ICECUBE version of the Antarctic Muon and Neutrino Detector Array (AMANDA) experiment at the South Pole, as well as the Radio Ice Cherenkov Experiment (RICE), which aims at measuring the radio pulse from the neutrino interac-

tion, the French Astronomy with a Neutrino Telescope and Abyss environmental RESearch (ANTARES) proposal, and the NESTOR project in the Mediterranean.

An alternative method is to search for extensive air showers initiated by electrons produced by neutrinos via the charged current process. The interaction length of cosmic ray hadrons and *gamma*-rays is smaller than $\sim 100 \, \mathrm{g \, cm}^{-2}$ above 10 EeV, even if uncertainties and fluctuations are taken into account, and the probability of these strongly interacting particles initiating air showers deeper than $1500 \, \mathrm{g \, cm}^{-2}$ is therefore negligibly small. Thus, showers starting deep in the atmosphere must be produced by penetrating particles such as neutrinos. Large neutrino detectors for measuring HECR air showers using the air fluorescence technique, such as the High Resolution Fly's Eye now under construction [57] or the planned Japanese Telescope Array [58], will have the potential to search for deeply penetrating showers (DPSs) initiated by neutrinos [28]. Their resolution of measurement of the atmospheric depth at which the shower has its maximum particle density is expected to be less than $30 \, \mathrm{g \, cm}^{-2}$ and the discrimination between DPSs and the regular air showers would be relatively straightforward. A possible contamination by a potential background of DPSs, secondary showers that result from tau lepton decays deep in the atmosphere or from γ-ray bremsstrahlung by muons, has been estimated to be less than 10^{-3} for 10 yr observation by a typical fluorescence detector. Hence UHE neutrino astronomy with air fluorescence detectors is not background limited [28].

In addition, a giant surface array such as the proposed Pierre Auger project [42] also has significant sensitivity for neutrino detection by search for horizontal air showers. The recently proposed satellite observatory concept for an Orbiting Wide-angle Light collector (OWL) [44] would increase the sensitivity to horizontal air showers by at least another order of magnitude.

Detection rates can be obtained by folding the predicted fluxes with the product of the charged current neutrino-nucleon cross section for which we use the recent parametrization $\sigma_{\nu N}(E) \simeq 2.82 \times 10^{-32} (E/10 \, \mathrm{EeV})^{0.402} \, \mathrm{cm}^2$ [59] and the acceptance $A(E)$. Since the astrophysical ''background'' from other sources of UHE neutrinos, most notably active galactic nuclei and Gamma Ray Bursts [60,61], and the secondary neutrinos produced by photopion production by HECR [28] is expected to be negligible above 10 EeV, we present integral event rates for neutrinos above 10 EeV in Fig. 5 for the viable HECR explaining TD models from Table I. We furthermore assume an acceptance scaling as $A(E) \propto E^{0.25}$ which seems to be implied by experimental studies.

For a given m_X, the maximum of the neutrino event rates over all decay modes except the ones only involving neutrinos is typically reached for the pure quark decay modes, except for $m_X = 10^{13}$ GeV, where the $l\nu$ mode produces the highest rates. As can be seen from Fig. 5, for all m_X this maximum actually saturates the general bound on the integral neutrino detection rate $R(E)$ pointed out in Ref. [13],
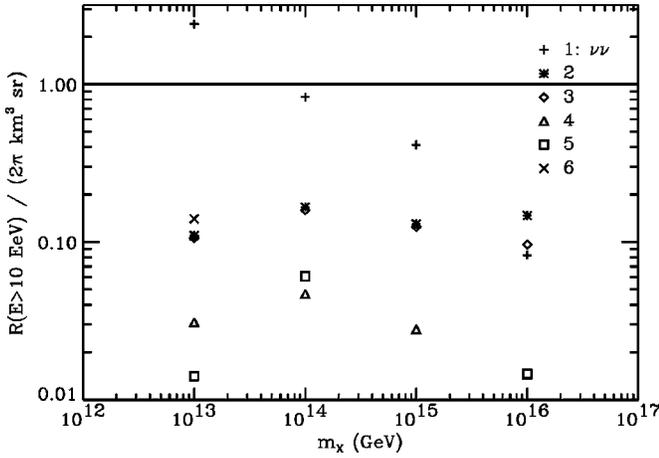
FIG. 5. Maximal event rates for muon neutrinos and anti-neutrinos in a detector of $2\pi\,\mathrm{km}^3$ sr acceptance for the viable scenarios from Table I, ordered by row number for given m_X. Electron neutrino event rates are about a factor of 2 smaller. The rates for tau neutrinos are at least a factor of 100 smaller still, except if produced directly in the decay. The telescope array is roughly sensitive to the range above the horizontal line, assuming a duty cycle of 10% and a lifetime of 10 yr.

$$R(E) \lesssim 0.34 r \left[\frac{A(E)}{2\pi\,\mathrm{km}^3\,\mathrm{sr}} \right] \left(\frac{E}{10^{19}\,\mathrm{eV}} \right)^{-0.6} \mathrm{yr}^{-1}, \qquad (2)$$

for $E \gtrsim 1$ PeV, where r is the ratio of energies injected into the neutrino versus EM channel. This is not surprising because for all decay modes except the ones only involving neutrinos, $r \lesssim 0.5$. The constraint, Eq. (2), is independent of the FF and arises from comparing the energy content in neutrinos and γ-rays, the latter being bounded from above by the EGRET measurement.

The highest possible rates are reached for the exclusive neutrino decay mode at $m_X = 10^{13}$ GeV for which the bound, Eq. (2), is not applicable because $r = \infty$, and the relevant quantity is the fraction of energy produced as secondary γ-rays instead. As can be seen from Fig. 4, the neutrino flux continues down to $\sim 10^{15}$ eV in these scenarios and can be comparable to fluxes predicted by models of active galactic nuclei [60,61]. The maximally possible event rates from muon neutrinos above 1 PeV per year in a $2\pi\,\mathrm{km}^3$ sr detector are $\simeq 5.5$ for $m_X = 10^{13}$ GeV and $\simeq 3.5$ for $m_X = 10^{14}$ GeV.

In general, we conclude that at least the highest rates predicted by TD models should be observable by next generation experiments such as the Pierre Auger Observatory and especially the OWL project, as can also be seen from the sensitivities shown in the figures.

VI. SUMMARY

Apart from the decay spectra and rates, the uncertainty of flux predictions in TD scenarios is governed by astrophysical uncertainties, mainly the universal radio background and the large scale extragalactic magnetic field. Our calculations show, however, that for most combinations of likely values for these astrophysical parameters and the energy scale of new physics, there are possible decay modes and fragmentation functions that lead to scenarios explaining the highest energy cosmic rays above the GZK cutoff, and some of them even down to $\simeq 10$ EeV, without violating observational constraints on γ-ray and neutrino fluxes. For example, an X particle of mass $m_X \simeq 10^{16}$ GeV decaying into quarks with a fragmentation function motivated by supersymmetry can explain cosmic rays above $\simeq 20$ EeV for an EGMF $> 10^{-10}$ G. This scenario predicts a transition from a nucleon dominated component to an about equal mixture of nucleons and γ-rays above $\simeq 100$ EeV in the case of a relatively strong universal radio background and a large scale magnetic field $\lesssim 10^{-10}$ G, a signature that should be testable within the next few years. Other tests involve GeV γ-rays whose flux comes close to the EGRET measurement and ultra high energy neutrino fluxes that should be detectable by $\gtrsim$ few km scale neutrino observatories which are now in the planning stage.

Another interesting viable class of scenarios involves pure neutrino decay modes in the context of eV neutrino masses which can yield even higher neutrino event rates up to a few per year in km scale detectors above $\simeq 10$ EeV for $m_X \lesssim 10^{14}$ GeV. The neutrino flux extends down to ~ 1 PeV in these models where it can be comparable to predictions from models of active galactic nuclei. Furthermore, for a modest amount of clustering of neutrino dark matter on the scale of the local Supercluster, secondary γ-ray and nucleon production by neutrino interactions with the clustered component can provide a significant fraction of the highest energy cosmic ray flux.

[1] D. J. Bird *et al.*, Phys. Rev. Lett. **71**, 3401 (1993); Astrophys. J. **424**, 491 (1994); **441**, 144 (1995).

[2] N. Hayashida *et al.*, Phys. Rev. Lett. **73**, 3491 (1994); S. Yoshida *et al.*, Astropart. Phys. **3**, 105 (1995); M. Takeda *et al.*, Phys. Rev. Lett. **81**, 1163 (1998).

[3] For a review see, e.g., R. Blandford and D. Eichler, Phys. Rep. **154**, 1 (1987).

[4] A. M. Hillas, Annu. Rev. Astron. Astrophys. **22**, 425 (1984).

[5] K. Greisen, Phys. Rev. Lett. **16**, 748 (1966); G. T. Zatsepin and V. A. Kuzmin, Pisma Zh. Eksp. Teor. Fiz. **4**, 114 (1966)

[JETP Lett. **4**, 78 (1966)].

[6] G. Sigl, D. N. Schramm, and P. Bhattacharjee, Astropart. Phys. **2**, 401 (1994); J. W. Elbert and P. Sommers, Astrophys. J. **441**, 151 (1995).

[7] J. L. Puget, F. W. Stecker, and J. H. Bredekamp, Astrophys. J. **205**, 638 (1976); L. N. Epele and E. Roulet, J. High Energy Phys. **10**, 009 (1998); F. W. Stecker and M. H. Salamom, astro-ph/9808110, Astrophys. Lett. (to be published).

[8] P. Bhattacharjee, C. T. Hill, and D. N. Schramm, Phys. Rev. Lett. **69**, 567 (1992).

[9] X. Chi *et al.*, Astropart. Phys. **1**, 129 (1993); **1**, 239 (1993).

[10] G. Sigl, K. Jedamzik, D. N. Schramm, and V. Berezinsky, Phys. Rev. D **52**, 6682 (1995).

[11] R. J. Protheroe and P. A. Johnson, Astropart. Phys. **4**, 253 (1996).

[12] R. J. Protheroe and T. Stanev, Phys. Rev. Lett. **77**, 3708 (1996); **78**, 3420(E) (1997).

[13] G. Sigl, S. Lee, D. N. Schramm, and P. S. Coppi, Phys. Lett. B **392**, 129 (1997).

[14] A. J. Gill and T. W. B. Kibble, Phys. Rev. D **50**, 3660 (1994).

[15] C. T. Hill, Nucl. Phys. **B224**, 469 (1983).

[16] P. Bhattacharjee and G. Sigl, Phys. Rev. D **51**, 4079 (1995).

[17] V. Berezinsky and A. Vilenkin, Phys. Rev. Lett. **79**, 5202 (1997).

[18] G. Vincent, N. D. Antunes, and M. Hindmarsh, Phys. Rev. Lett. **80**, 2277 (1998).

[19] J. N. Moore and E. P. S. Shellard, hep-ph/9808336.

[20] P. Bhattacharjee, Q. Shafi, and F. W. Stecker, Phys. Rev. Lett. **80**, 3698 (1998).

[21] U. F. Wichoski, J. H. MacGibbon, and R. H. Brandenberger, hep-ph/9805419.

[22] Yu. L. Dokshitzer, V. A. Khoze, A. H. Müller, and S. I. Troyan, *Basics of Perturbative QCD* (Editions Frontières, Singapore, 1991).

[23] V. Berezinsky and M. Kachelriess, Phys. Lett. B **434**, 61 (1988).

[24] M. Birkel and S. Sarkar, Astropart. Phys. **9**, 297 (1998).

[25] P. Bhattacharjee and N. C. Rana, Phys. Lett. B **246**, 365 (1990).

[26] S. Lee, Phys. Rev. D **58**, 043004 (1998).

[27] T. J. Weiler, Phys. Rev. Lett. **49**, 234 (1982); Astrophys. J. **285**, 495 (1984).

[28] S. Yoshida, Astropart. Phys. **2**, 187 (1994); S. Yoshida, H. Dai, C. C. H. Jui, and P. Sommers, Astrophys. J. **479**, 547 (1997).

[29] T. J. Weiler, hep-ph/9710431.

[30] S. Yoshida, G. Sigl, and S. Lee, Phys. Rev. Lett. (to be published), hep-ph/9808324.

[31] See, e.g., P. J. E. Peebles, *Principles of Physical Cosmology* (Princeton University Press, Princeton, 1993).

[32] F. A. Aharonian, P. Bhattacharjee, and D. N. Schramm, Phys. Rev. D **46**, 4188 (1992).

[33] T. A. Clark, L. W. Brown, and J. K. Alexander, Nature (London) **228**, 847 (1970).

[34] R. J. Protheroe and P. L. Biermann, Astropart. Phys. **6**, 45 (1996).

[35] P. P. Kronberg, Rep. Prog. Phys. **57**, 325 (1994).

[36] See, e.g., S. Biller *et al.*, Phys. Rev. Lett. **80**, 2992 (1998).

[37] G. Sigl, S. Lee, D. N. Schramm, and P. Bhattacharjee, Science **270**, 1977 (1995).

[38] M. A. Lawrence, R. J. O. Reid, and A. A. Watson, J. Phys. G **17**, 733 (1991).

[39] P. Sreekumar *et al.*, Astrophys. J. **494**, 523 (1998).

[40] W. Rhode *et al.*, Astrophys. J. **4**, 217 (1996).

[41] R. M. Baltrusaitis *et al.*, Astrophys. J. Lett **281**, 9 (1984); Phys. Rev. D **31**, 2192 (1985).

[42] K. S. Capelle, J. W. Cronin, G. Parente, and E. Zas, Astropart. Phys. **8**, 321 (1998).

[43] *Proceedings of the International Symposium on Extremely High Energy Cosmic Rays: Astrophysics and Future Observatories* (Institute for Cosmic Ray Research, Tokyo, 1996).

[44] J. F. Ormes *et al.*, in Proceedings of the 25th International Cosmic Ray Conference, Durban, 1997, edited by M. S. Potgieter *et al.* (unpublished), Vol. 5, p. 273; Y. Takahashi *et al.*, in *Proceedings of the International Symposium on Extremely High Energy Cosmic Rays: Astrophysics and Future Observation* [43], p. 310.

[45] M. H. Salamon and F. W. Stecker, Astrophys. J. **493**, 547 (1998).

[46] P. S. Coppi and F. A. Aharonian, Astrophys. J. Lett. **487**, 9 (1997).

[47] R. Arnowitt and P. Nath, Phys. Rev. Lett. **69**, 725 (1992); Phys. Rev. D **49**, 1479 (1994).

[48] D. J. H. Chung, E. W. Kolb, and A. Riotto, Phys. Rev. D **59**, 023501 (1999).

[49] V. Kuzmin and I. Tkachev, JETP Lett. **68**, 271 (1998); hep-ph/9809547.

[50] D. V. Nanopoulos, hep-ph/9809546.

[51] V. Kuzmin and V. A. Rubakov, Phys. At. Nucl. **61**, 1028 (1998).

[52] See, e.g., D. J. H. Chung, E. W. Kolb, and A. Riotto, Phys. Rev. Lett. **81**, 4048 (1998).

[53] V. Berezinsky, M. Kachelriess, and A. Vilenkin, Phys. Rev. Lett. **79**, 4302 (1997).

[54] V. Berezinsky, P. Blasi, and A. Vilenkin, Phys. Rev. D **58**, 103515 (1998).

[55] F. Halzen, R. A. Vazquez, T. Stanev, and H. P. Vankov, Astropart. Phys. **3**, 151 (1995).

[56] J. W. Cronin, in Proceedings of the International Workshop on Techniques to Study Cosmic Rays with Energies $\geqslant 10^{13}$ eV, edited by M. Boratav *et al.* [Nucl. Phys. B (Proc. Suppl.) **28B**, 213 (1992)].

[57] S. C. Corbató *et al.*, Nucl. Phys. B (Proc. Suppl.) **28B**, 36 (1992); M. Al-Seady *et al.*, in *Proceedings of the International Symposium on Extremely High Energy Cosmic Rays: Astrophysics and Future Observatories* [43], p. 191.

[58] M. Teshima *et al.*, Nucl. Phys. B (Proc. Suppl.) **28B**, 169 (1992); M. Hayashida *et al.*, in *Proceedings of the International Symposium on Extremely High Energy Cosmic Rays: Astrophysics and Future Observatories* [43], p. 205.

[59] R. Ghandi, C. Quigg, M. H. Reno, and I. Sarcevic, Astropart. Phys. **5**, 81 (1996); Phys. Rev. D **58**, 093009 (1998).

[60] See, e.g., F. Halzen and E. Zas, Astrophys. J. **488**, 669 (1997).

[61] See, e.g., E. Waxman and J. Bahcall, Phys. Rev. D (to be published), hep-ph/9807282.